SUPERFLUID AND NORMAL-FLUID DENSITY IN THE CUPRATE SUPERCONDUCTORS

D.B. Tanner[a], F. Gao[a], K. Kamarás[a], H.L. Liu[a], M.A. Quijada[a], D.B. Romero[a], Y-D. Yoon[a], A. Zibold[a], H. Berger[b], G. Margaritondo[b], L. Forró[b], R.J. Kelly[c], M. Onellion[c], G. Cao[d], J.E. Crow[d], Beom-Hoan O[e], J.T. Markert[e], J.P. Rice[f], D.M. Ginsberg[f], and Th. Wolf[g]

[a]University of Florida; [b]École Polytechnique Fédéral de Lausanne; [c]University of Wisconsin; [d]National High Magnetic Field Laboratory; [e]University of Texas; [f]University of Illinois; [g]Forschungszentrum Karlsruhe.

Abstract As carriers are introduced into the cuprates (by doping the insulating "parent" compounds) spectral weight appears in the optical spectrum at photon energies below the charge-transfer gap. This spectral weight increases as the doping level increases. Magnetic penetration depth measurements have shown a good correlation between superfluid density and superconducting transition temperature in the underdoped-to-optimally-doped part of the phase diagram. Optical measurements allow independent determination of the total doping-induced spectral weight and the superfluid density. These measurements, made on cuprates with transition temperatures from 40 to 110 K, find that in optimally doped materials only about 20% of the doping-induced spectral weight joins the superfluid. The rest remains in finite-frequency, midinfrared absorption. In underdoped materials, the superfluid fraction is even smaller. This result implies extremely strong coupling for these superconductors.

Keywords: superconductivity; infrared

INTRODUCTION

Essentially every conduction electron participates in the $T = 0$ superfluid of a clean metallic superconductor.[1,2] Compelling evidence for this claim is the penetration depth, which, when corrected for nonlocal effects, gives about the same electron density as the free-carrier optical plasma frequency ω_p, i. e., $\Lambda_L^{-2} = 4\pi n_s e^2/cm^* = \omega_{ps}/c$ with $\omega_{ps} \approx \omega_p$. Here, Λ_L is the London value for the penetration depth, n_s is the density of superconducting electrons and m^* their effective mass. The same superfluid density n_s enters the infinite dc conductivity of the superconductor: the inductive screening of electromagnetic waves is directly related (*via* the Kramers-Kronig integral) to the spectral weight or oscillator strength of the zero-frequency delta function in the optical conductivity. In what follows, we call the n_s extracted from either the penetration depth or the delta-function oscillator strength the "superfluid density."

Strong-coupled metallic systems exhibit a modest reduction in superfluid density on account of the Holstein phonon emission process,[3] where a charge carrier absorbs a photon of energy ω, emits an excitation of energy Ω, and scatters, giving rise to absorption. In a clean metal at zero temperature, this process is the dominant cause of infrared absorption, because it the principal mechanism by which the momentum of the charge carriers can be changed. This finite-frequency absorption removes oscillator strength from the delta function, and increases the penetration depth.

In metals, the excitation that is emitted is generally a phonon, but in fact it could be any boson that couples linearly to the charge carriers. The interaction leads to a frequency- and temperature-dependent scattering rate, given at high temperatures by $1/\tau = 2\pi\lambda T$, with λ the dimensionless electron-boson coupling constant. A related consequence of this interaction is a low-energy mass enhancement, which is governed by the same quantity λ. The effective mass m^* becomes $m^* = (1 + \lambda)m$, where m is the band mass. Because the low-energy penetration depth is proportional to m^*, the mass enhancement increases the penetration depth and reduces the weight of the delta function.

How do these ideas apply to the cuprate superconductors? The cuprate superconductors are generally believed to be in the clean, local limit, and thus to obey London electrodynamics. The reason for this belief is that the three *ab*-plane length scales are ordered as

(1) coherence length (ξ_{ab}~17 Å); (2) mean free path (ℓ_{ab}~100 Å), and hence in the clean limit; (3) penetration depth (λ_{ab}~1500 Å), and therefore local electrodynamics. Consequently, the cuprates, even with a *d*-wave gap, should have most of the superconducting-state spectral weight or oscillator strength in the zero-frequency delta-function.

As will be seen in a moment, most of the spectral weight of the doped carriers is *not* in the delta function; instead, it remains in the broad "midinfrared" spectrum. The presence of this absorption has been known since the early days of the cuprate materials. Three things motivate a reexamination of the spectral weight at this time: (1) The fraction of the spectral weight in the superfluid is small, suggesting an extremely strongly coupled system. (2) The fraction in the superfluid is about 20–25% for *all* optimally-doped systems. (3) In underdoped materials, the superfluid fraction is reduced further.

OPTICAL TECHNIQUES

Normal-incidence, polarized reflectance $\mathscr{R}$ was measured by using a Bruker IFS-113v Fourier transform spectrometer (80–4000 cm^{-1}) in the far-infrared and midinfrared region and a modified Perkin-Elmer 16U grating spectrometer in the near-infrared and ultraviolet (2000–33,000 cm^{-1}). We used wire grid polarizers in the far–midinfrared and dichroic polarizers in the near infrared–ultraviolet. Low-temperature measurements (10–300 K) employed a continuous-flow cryostat.

The measurement process consisted of obtaining spectra at each temperature for both the sample and for a reference Al mirror. Their ratio gives a preliminary reflectance of the sample. After completing these measurements at each temperature for each polarization, the proper normalizing of the reflectance was obtained by taking a final room temperature spectrum, coating the sample with 2000 Å of Al, and remeasuring this coated surface. The ratio of the spectrum from the uncoated sample to the reflectance of the coated surface was multiplied by the known reflectance of Al to give the most accurate result for the room-temperature reflectance. This result was then used to correct the reflectance data measured at other temperatures by comparing the individual room-temperature spectra taken in the two separate runs. This procedure compensates for any misalignment between the sample and the mirror used as a temporary reference

before the sample was coated, corrects for interference in the cryostat window, and, most importantly, provides a reference surface of the same size and profile as the actual sample.

The uncertainties in the absolute value of the reflectance are in the order of ±1%. This uncertainty is in good agreement with the reproducibility found from the measurements of different samples.[4] It leads to an uncertainty in the conductivity which varies with frequency, equal to $\pm 1\%(\mathscr{R}/(1-\mathscr{R}(\omega)^2)$.

KRAMERS-KRONIG ANALYSIS

We estimated the optical constants by Kramers-Kronig transformation of the reflectance data.[5] The low- and high-frequency extrapolations were done in the following way. We extended the low-frequency data using a Lorentz-Drude model, dominated at the low frequencies by the free-carrier (Drude) form. Finite-frequency excitations are modeled by Lorentz oscillators. In the superconducting state, the reflectance is expected to be unity for frequencies close to zero, and we used the same Lorentz-Drude model, but with the Drude scattering rate set to zero.

We extended the high-frequency end using data from the literature where available, and then using $\mathscr{R}(\omega) \sim \omega^{-s}$ up to a crossover frequency ω_f and $\mathscr{R}(\omega) \sim \omega^{-4}$ thereafter. The exponent s is a number that can be between 0 and 4; we used $s \sim 1$. The crossover frequency was chosen to be $\sim 1,000,000\ \mathrm{cm}^{-1}$ (125 eV) We observed some dependence of the results on the choice of s and ω_f for frequencies close to the highest frequencies. For frequencies below 20,000 cm^{-1}, however, the effects of this choice were insignificant.

OPTICAL CONDUCTIVITY

The optical conductivity at two temperatures for the a-axis of a $Bi_2Sr_2CaCu_2O_8$ single crystal is shown in Fig. 1. In the normal state (100 K), the low-frequency optical conductivity extrapolates reasonably well to the dc conductivity. The temperature dependence[4,6] agrees with the T-linear resistivity; and, there is a characteristic narrowing of this far-infrared portion of the spectrum. In contrast, $\sigma_1(\omega)$ does not show much temperature variation at high frequencies; the curves draw together around 3000 cm^{-1}. Below T_c, the low-frequency conductivity is considerably reduced. The "missing

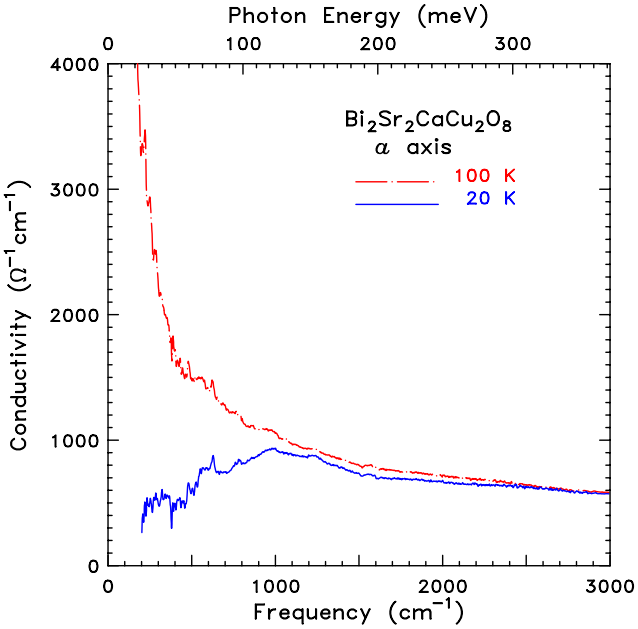

Fig. 1. Optical conductivity for the a-axis of $Bi_2Sr_2CaCu_2O_8$.

area" in the far-infrared conductivity appears as the zero-frequency delta-function response of the superfluid. This aspect is discussed in more detail in the next section.

SUM RULE ANALYSIS

The doping of insulating cuprates introduces mobile carriers into the CuO_2 planes, increasing the low energy spectral weight and decreasing the oscillator strength of the 1.5–2 eV charge-transfer band.[7–10] Infrared spectroscopy may be used to estimate the doping-induced spectral weight, using the partial sum rule for the optical conductivity.[5]

$$N_{eff}(\omega)\frac{m}{m^*} = \frac{2mV_{\rm cell}}{\pi e^2}\int_0^{\omega}\sigma_1(\omega')d\omega' \qquad (1)$$

where e and m are the free-electron charge and mass respectively, m^* the effective mass, and $V_{\rm cell}$ the volume occupied by one formula unit. For simplicity, we will take $m^* = m$ in the rest of this discussion and consider $N_{eff}(\omega)$ to represent the effective number of carriers per formula unit participating in optical transitions below frequency ω.

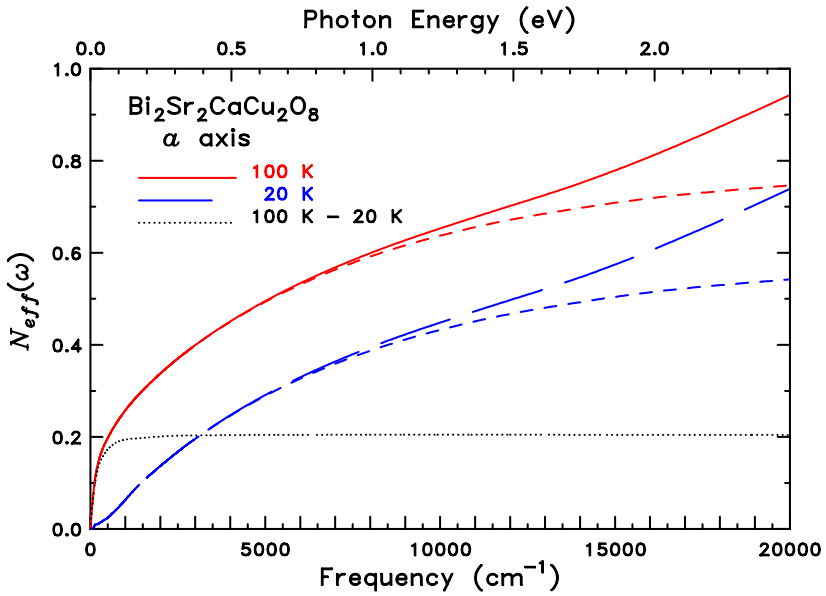

Fig. 2. Partial sum rule for the a-axis of $Bi_2Sr_2CaCu_2O_8$.

Figure 2 shows as the upper (solid) curves N_{eff} for the a-axis of a single-domain $Bi_2Sr_2CaCu_2O_8$ crystal at $T = 100$ K.[6] The curve rises, begins to flatten out, and then increases slope at the onset of the charge-transfer band. The short dashed line is obtained by subtracting from $\sigma_1(\omega)$ the contributions of the charge-transfer and higher-lying bands (obtained by a fit of the data to a Drude-Lorentz model) before integration. The value at which the 100 K dashed line saturates is a good estimate of N_{eff}.

The optical conductivity may be used to estimate the superfluid density, N_s, in two ways. First, one may evaluate $N_{eff}(\omega)$ for $T < T_c$. The data table for $\sigma_1(\omega)$ naturally omits the zero-frequency infinite dc conductivity; thus the numerical integral misses the delta-function contribution, and the "missing area" in $N_{eff}(\omega)$ below T_c gives the superfluid density. Figure 2 shows (as the long dashed curves) N_{eff} at 20 K for the a-axis of a single-domain $Bi_2Sr_2CaCu_2O_8$ crystal.[6] The 20 K data are nearly parallel to the 100 K data; the dotted line is the difference between them, and is an estimate of N_s.

The second method used to estimate the superfluid density considers the inductive response of the superfluid. One may look at the imaginary part of $\sigma(\omega)$, at the real part of the dielectric function, $\epsilon_1(\omega)$, or at a generalized London penetration depth, $\Lambda_L(\omega)$. For a

delta-function $\sigma_1(\omega)$, one may write

$$\Lambda_L(\omega) = \frac{c}{\omega\sqrt{1-\epsilon_1(\omega)}} \tag{2}$$

(Note that this can also be written in terms of the imaginary part of the conductivity, $\sigma_2(\omega)$, as $\Lambda_L = c/\sqrt{4\pi\omega\sigma_2(\omega)}$. One finds[6,11,12] that the function $\Lambda_L(\omega)$ is nearly flat in the far infrared, and in agreement with μSR[13] and other measurements made at $\omega = 0$. From Λ_L one may pass directly to the number of superfluid electrons, $N_s = n_s V_{\rm cell}$.

Both methods agree relatively well ($\pm 5\%$), implying that there is no conflict between the "missing area" in the far-infrared optical conductivity and the superfluid density inferred from the penetration depth so far as the *ab* plane goes. In this the *ab* plane is quite different (and more conventional) than the recent results for light polarized along the *c* axis.[14] In the latter measurement, the far-infrared missing area could only account for about half of the delta-function area and a transfer of spectral weight from very high energies to the superfluid was invoked.

As a check of these analyses, one may also make a fit of a Drude-Lorentz model to the data and get N_{eff} from the sum of the squares of the plasma frequencies of the Drude and those Lorentzians with center frequencies below the charge-transfer gap. Then, with the superconducting response modeled by collapsing the Drude scattering rate to zero, the Drude response gives the superfluid density. This modeling produces carrier densities also within about 5% of those obtained by the other methods.

DISCUSSION

Figure 3 shows the results for single crystals of a number of materials. The left panel shows a "Uemura plot,[13]" displaying T_c as a function of the *ab*-plane superfluid density. (The superfluid density is expressed as carriers per copper atom in order to allow for the differing number of Cu layers and differing interlayer spacing in the materials studied; however a plot as a function of 3-dimensional carrier density looks very similar.[15]) The typical linear increase of T_c with superfluid density is clearly seen.

The right panel is similar. It shows T_c as a function of the *total* doping-induced carrier density, N_{eff}. The linear increase of T_c with

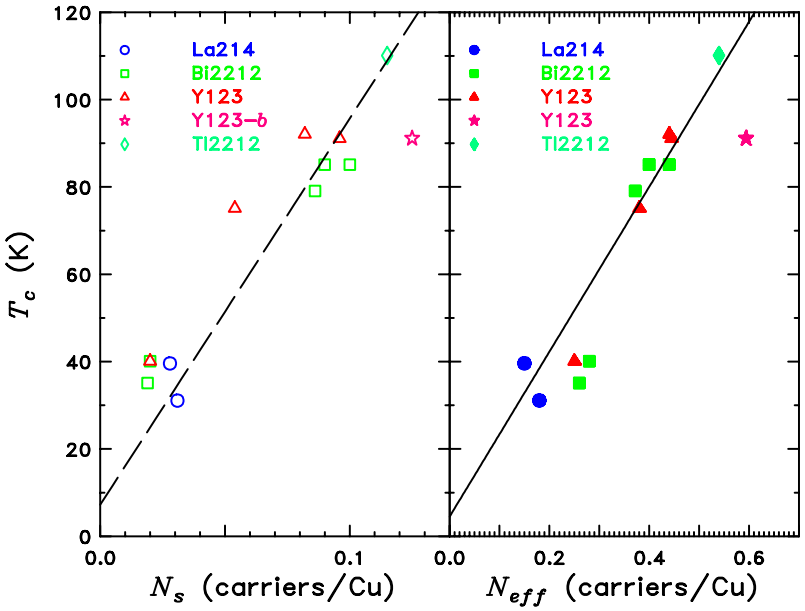

Fig. 3. Left panel: $T_c$as a function of the superfluid density. Right panel: T_c as a function of the total doping-induced spectral weight. The lines are least square fits to the data for optimally doped crystals.

total carrier density is clearly seen. The difference between the two panels is that the horizontal scale of the right-hand plot is five times that of the left-hand plot, implying that only about 1/5 of the doped-in carriers join the superfluid. This ratio holds quite closely for all optimally-doped materials, from $T_c = 40$ K $La_2CuO_{4+\delta}$ to $T_c = 110$ K $Tl_2Ba_2CaCu_2O_8$. It even works reasonably well for the b axis of $YBa_2Cu_3O_7$ (represented by the stars in the figure) for which we have assumed 3 coppers per formula unit. For underdoped materials the ratio N_s/N_{eff} becomes smaller and smaller as the doping level decreases from the optimum amount.

There are other implications of this result. For example, in the standard model, cuprate infrared conductivity is associated with a strong frequency-dependence to the quasiparticle scattering rate, $1/\tau(\omega, T)$. This picture was first presented in the context of the marginal Fermi liquid[16] and nested Fermi liquid pictures[17] pictures but also occurs in the d-wave theories of the superconductivity.[18,19] This picture has a difficult task to account for small value of the superfluid spectral weight. Because these materials are in the clean

limit, the only way that the carriers can absorb light is through a process in which the emission of some excitation occurs.[20–22] As already mentioned, the oscillator strength in this Holstein sideband and the enhancement of the condensate effective mass is a measure of the interaction strength between the carriers and the excitation, λ. Using ${\omega_{ps}}^2 = 4\pi n_s e^2/m^*$ with $m^* = (1+\lambda)m$, a reduction of the superfluid oscillator strength by a factor of 5 implies $\lambda = 4$. This value represents extremely strong coupling; moreover it is not consistent with the value $\lambda = 0.3$ inferred from the temperature or frequency dependence of $1/\tau(\omega, T)$.[6,23,24]

ACKNOWLEDGMENTS

We would like to acknowledge many discussions with P.J. Hirschfeld. Work at Florida was supported by the NSF—Solid State Physics—through grant number DMR-9705108. Research at the EPFL has received support from the Swiss National Science Foundation, at Wisconsin from the DOE, at the National High Magnetic Field Laboratory from NSF Cooperative Agreement No. DMR-9527035 and the State of Florida, at Texas from NSF Grant DMR-9158089, and at Illinois from NSF Grant DMR-9120000 through the Science and Technology Center for Superconductivity.

REFERENCES CITED

1. A.B. Pippard, *Proc. Roy. Soc. (London)* **A216**, 547 (1953).
2. M. Tinkham, *Introduction to Superconductivity, Second Edition*, (McGraw-Hill, New York, 1996).
3. P.B. Allen, *Phys. Rev. B* **3**, 305 (1971).
4. M.A. Quijada, D.B. Tanner, R.J. Kelley and M. Onellion, *Z. Phys. B* **94**, 255 (1994).
5. Frederick Wooten, *Optical Properties of Solids* (Academic Press, New York, 1972).
6. M.A. Quijada, D.B. Tanner, R.J. Kelley, M. Onellion, and H. Berger, *Phys. Rev. B* **60**, 14000 (1999).
7. S.L. Cooper, G.A. Thomas, J. Orenstein, D.H. Rapkine A.J. Millis, S.-W. Cheong, A.S. Cooper, and Z. Fisk, *Phys. Rev. B* **41**, 11 605 (1990).
8. S. Uchida, T. Ido, H. Takagi, T. Arima, Y. Tokura, and S. Tajima, *Phys. Rev. B* **43**, 7942 (1991).

9. M.B.J. Meinders, H. Eskes and G.A. Sawatzky, *Phys. Rev. B* **48**, 3916 (1993).
10. H. Eskes, A.M. Oles, M.B.J. Meinders, and W. Stephan, *Phys. Rev. B* **50**, 17 980 (1994).
11. D.N. Basov, R. Liang, D.A. Bonn, W.N. Hardy, B. Dabrowski, M. Quijada, D.B. Tanner, J.P. Rice, D.M. Ginsberg, and T. Timusk, *Phys. Rev. Lett.* **74**, 598 (1995).
12. M.A. Quijada, D.B. Tanner, F.C. Chou, D.C. Johnston, and S-W. Cheong, *Phys. Rev. B* **52**, 15 485 (1995).
13. Y.J. Uemura, L.P. Le, G.M. Luke, B.J. Sternlieb, W.D. Wu, J.H. Brewer, T.M. Riseman, C.L. Seaman, M.B. Maple, M. Ishikawa, D.G. Hinks, J.D. Jorgensen, G. Saito, and H. Yamochi, *Phys. Rev. Lett.* **66**, 2665 (1991).
14. D.N. Basov, S.I. Woods, A.S. Katz, E.J. Singley, R.C. Dynes, M. Xu, D.G. Hinks, C.C. Homes, and M. Strongin, *Science* **283**, 49 (1999).
15. H.L. Liu, M.A. Quijada, A. Zibold, Y.-D. Yoon, D.B. Tanner, G. Cao, J.E. Crow, H. Berger, G. Margaritondo, L. Forró, Beom-Hoan O, J.T. Markert, R.J. Kelly, and M. Onellion, *J. Phys.: Condens. Matter* **11**, 239 (1999).
16. C.M. Varma, P.B. Littlewood, S. Schmitt-Rink, E. Abrahams, and A.E. Ruckenstein, *Phys. Rev. Lett.* **63**, 1996 (1989).
17. A. Virosztek and J. Ruvalds, *Phys. Rev. B* **42**, 4064 (1990).
18. P.J. Hirschfeld, W.O. Puttika, and P. Wölfle, *Phys. Rev. Lett.* **69**, 1447 (1992).
19. S.M. Quinlan, P.J. Hirschfeld, and D.J. Scalapino, *Phys. Rev. B* **53**, 8775 (1996).
20. T. Holstein, *Phys. Rev.* **96**, 535 (1954).
21. J. Orenstein, S. Schmitt-Rink, and A.E. Ruckenstein, in *Electronic Properties of High-T_c Superconductors and Related Compounds,* ed. H. Kuzmany, M, Mehrig, J. Fink (Springer-Verlag, Berlin-Heidelberg, 1990).
22. P.B. Littlewood and C.M. Varma, *J. Appl. Phys.* **69**, 4979 (1991).
23. S.L. Cooper, A.L. Kotz, M.A. Karlow, M.V. Klein, W.C. Lee, J. Giapintzakis, and D.M. Ginsberg, *Phys. Rev. B* **45**, 2549 (1992).
24. D.B. Romero, C.D. Porter, D.B. Tanner, L. Forro, D. Mandrus, L. Mihaly, G.L. Carr, and G.P. Williams, *Solid State Commun.* **82**, 183 (1992).